Water Practice & Technology

IWA PUBLISHING

Water Practice & Technology Vol 17 No 1, 517 doi: 10.2166/wpt.2021.130

Photocatalytic degradation of caffeine in a slurry reactor with intermittent UV irradiation: optimization and response surface modelling

C. Nirmala Rani

Department of Civil Engineering, Jerusalem College of Engineering, Pallikaranai, Chennai 600100, India
E-mail: nirmalacrani@gmail.com

CN, 0000-0001-7970-7604

ABSTRACT

This study focusses on the photocatalytic degradation of caffeine (CAF), a stimulating drug and environmental contaminant that poses a threat to humans and the environment. The effect of operating parameters such as CAF initial concentration (5–20 mg/L), catalyst dosage (0.1–0.9 g/L) and pH (3.0–9.0) were explored in detail. The experimental results showed the maximum CAF and chemical oxygen demand (COD) removals of 87.2% and 66.7% respectively. The optimized parameters were: CAF initial concentration – 5 mg/L, catalyst dosage – 0.5 g/L and pH – 7.2. The photocatalytic degradation of CAF followed pseudo-first order kinetics. The obtained experimental data were analysed with response surface methodology (RSM) using Design Expert Software.

Key words: caffeine, COD, photocatalysis, TiO_2

HIGHLIGHTS

- The optimized parameters were: [CAF]=5 mg/L, [TiO_2]=0.5 g/L, pH=7.2.
- The maximum CAF and COD removals were 86.7 and 66.7% respectively.
- CAF and COD removals followed pseudo-first-order kinetics.
- Good agreement between experimental and predicted data.
- All operating parameters were significant in CAF and COD removals.

GRAPHICAL ABSTRACT

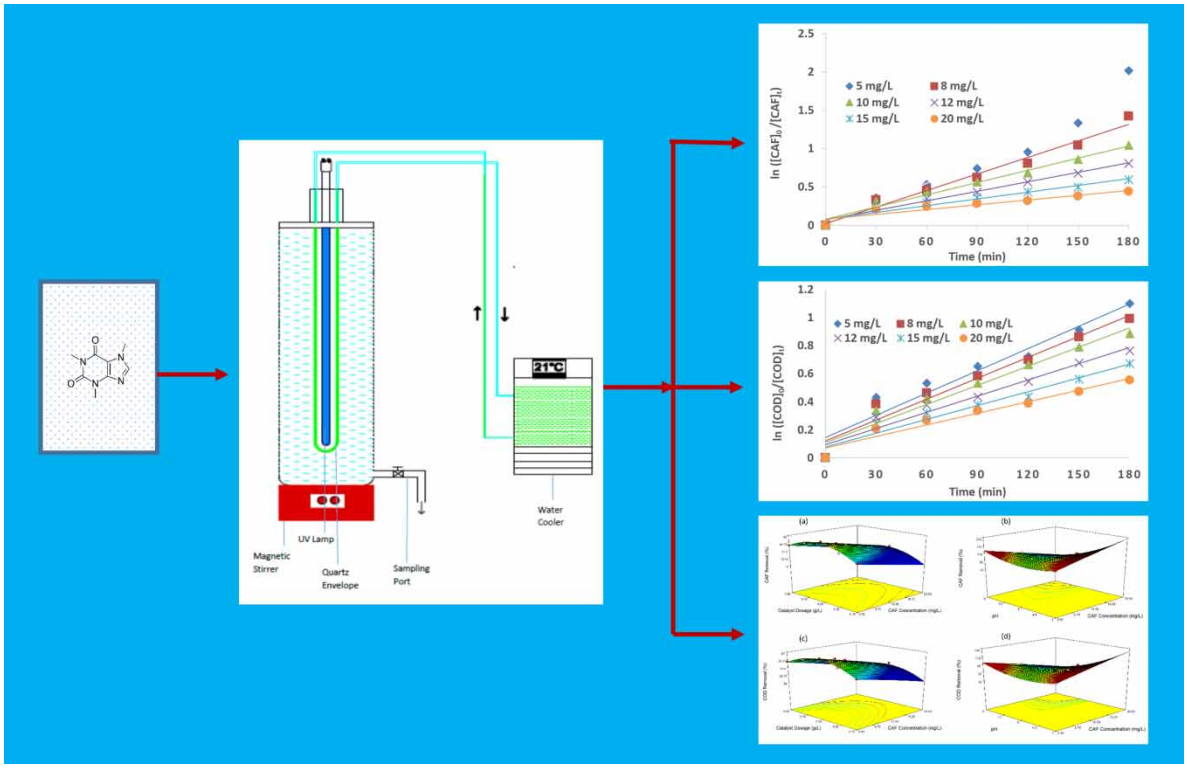

1. INTRODUCTION

Pharmaceutical and personal care products (PPCPs) in the aquatic environment are of environmental concern and have received more attention among the researchers due to their persistence and non-biodegradability (Fathinia & Khataee 2015). PPCPs occur in the aquatic environment because of industrial and municipal wastewater discharges. Even though their concentration is usually at the nanogram level in wastewater, they have toxic impact on both humans and in the environment. Since PPCPs are persistent and non-biodegradable, their removal is of great concern (Barcelo & Petrovic 2008).

Caffeine ($C_8H_{10}N_4O_2$), a PPCP and persistent organic pollutant (POP), is a psychoactive drug consumed widely across the globe (Lovett 2005) and found in beverages like coffee, tea, and soft and energy drinks, as well as food products including chocolate and ice cream, and some medicines (Miners & Birkett 1996; Indermuhle *et al.* 2013; Marques *et al.* 2013; Ghosh *et al.* 2019). Caffeine has high water solubility (Ks >10,000 mg/L) (Elhalil *et al.* 2018), a low octanol water partition coefficient (Log $K_{ow} = -0.07$) and a long half-life (Edwards *et al.* 2015). Even though short-term exposure to CAF is not a threat to living things (Moore *et al.* 2008), its intense use can cause mutation, anxiety, tremors (Zhang *et al.* 2011) and cardiovascular diseases (Torres *et al.* 2014; Elhalil *et al.* 2018).

Various methods including chlorination (Gould & Richards 1984), photo-Fenton (Klamerth *et al.* 2010; Trovo *et al.* 2013), ozonation (Rosal *et al.* 2008; Souza & Feris 2015), UV photolysis (Shu *et al.* 2013) and semiconductor-based heterogeneous photocatalysis (Marques *et al.* 2013; Arfanis *et al.* 2017; Elhalil *et al.* 2018; Luna *et al.* 2018; Vaiano *et al.* 2018) have been investigated for CAF degradation in aqueous solutions. UV photolysis is ineffective for CAF removal (Buerge *et al.* 2003), other methods – for example, ozonation, photo-Fenton and chlorination – are limited by slow reaction rates (Indermuhle *et al.* 2013; Ghosh *et al.* 2019).

Heterogeneous photocatalysis is an advanced oxidation process (AOP) applied to degrade POPs and found to be effective (Zhou *et al.* 2017; Elhalil *et al.* 2018). When a semiconductor absorbs a photon energy ($h\nu$) ≥ the semi-conductor band gap (Eg), an electron (e^-) may be promoted from the valence band (VB) to the conduction band (CB), thereby creating an electron vacancy – 'hole' (h^+) (Bahnemann *et al.* 1997; Fujishima *et al.* 2008; Gaya & Abdullah 2008). The electron and hole can migrate to the catalyst surface where they participate in redox

reactions with the species adsorbed on the catalyst surface. The holes can oxidize H_2O and OH^- to generate hydroxyl radicals ($^{\bullet}OH$) whereas the electrons, while reacting with oxygen, can reduce molecular oxygen O_2 to $O_2^{\bullet-}$ (Mozia 2010; Laohaprapanon *et al.* 2015; Puga 2016). The $^{\bullet}OH$ generated destroys the POPs, breaking them down into the relatively less toxic end products, CO_2 and H_2O (Diaz-Uribe *et al.* 2014). Among the semi-conductors applied as photocatalysts, such as TiO_2, ZnO, Fe_2O_3, WO_3, SnO_2, and ZrO_2 (Sudha & Sivakumar 2015; Ahmad *et al.* 2016; Awfa *et al.* 2018; Pathakoti *et al.* 2018), TiO_2 had attracted many researchers and been found successful due to its easy availability, low cost, non-toxicity, chemical and thermal stability, and applicability to solar energy (Bouarioua & Zerdaoui 2017; Rimoldi *et al.* 2017; Muangmora *et al.* 2020; Sujatha *et al.* 2020). As far as is known, no study has been conducted on CAF degradation using intermittent UV irradiation.

The objective of this study was to evaluate CAF photocatalytic degradation using intermittent irradiation from a 365 nm UV lamp (1 hour on and 10 minutes off for a trial period of 3 h 30 min) in a batch-scale reactor. Experiments were conducted in order to assess the effect of pH, TiO_2 dose, and initial CAF concentration for CAF removal. Photocatalytic degradation kinetics were also studied. Response surface methodology (RSM) using central composite design (CCD) was used to analyse the individual and interactive effects of operating variables on CAF and chemical oxygen demand (COD) removals.

2. METHODS

2.1. Materials

Caffeine ($C_8H_{10}N_4O_2$, MW-194.19 g/mol) and titanium dioxide (Evonik Degussa P25, Germany TiO_2, 21 nm TEM size) were purchased from Sigma Aldrich. The specific surface of the TiO_2 photocatalyst was 50 m^2/g, its band gap was 3.2 eV and it was a mixture of anatase (70%) and rutile (30%). Sodium hydroxide (99%), hydrochloric acid (36.5 to 38.0%), dichloromethane, acetonitrile and hexane, all of HPLC grade, came from Merck. COD determination was done using double-distilled water.

2.2. Experimental setup

Figure 1 is a schematic of a laboratory-scale, batch photocatalytic reactor. The reactor, made of Plexiglas, had a working volume of 2 L. A 16 W, 365 nm, low pressure, Hg UV-A lamp was used. The lamp was in the centre of

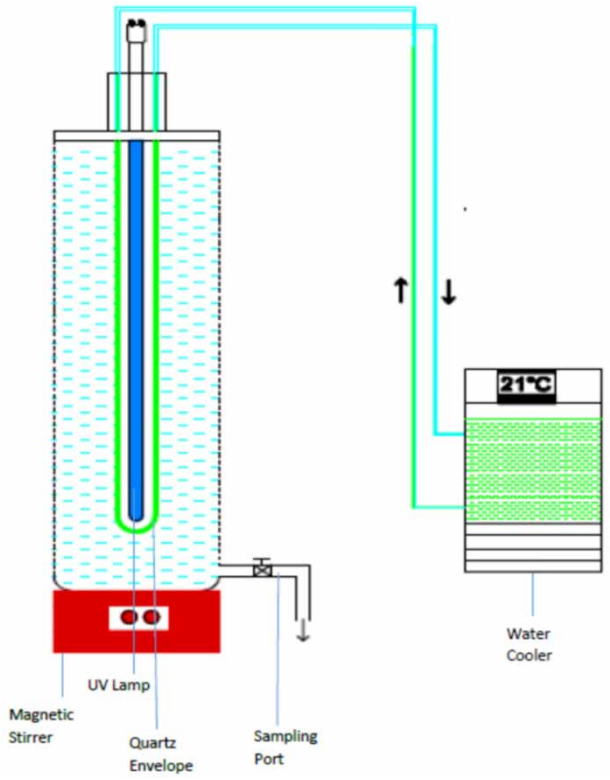

Figure 1 | Photocatalytic reactor.

the reactor so that irradiation was uniform and was enclosed in a double-layered, quartz glass envelope. Water was recirculated through the envelope to prevent the lamp causing thermo-catalytic effects.

2.3. Experimental procedure

The reaction mixture was prepared by adding known concentrations of CAF and the photocatalyst to distilled water. Before UV irradiation, the mixtures were stirred vigorously for 30 minutes in the dark, to establish an adsorption/desorption equilibrium on the photocatalytic surfaces. Subsequently, the mixture was stirred under UV irradiation. Sample aliquots were collected at 30 minute intervals and filtered to remove the solid particles. The CAF concentrations in the filtrates were determined using an INFRA DIGI IR513C Digital single beam UV-VIS Spectrophotometer (Gaurav Scientific Chemical, Raipur, India) at 273 nm. Proportional removal was calculated using Equation (1).

$$\text{Removal (\%)} = \frac{\text{Initial concentration} - \text{Final concentration}}{\text{Initial concentration}} \times 100 \quad (1)$$

2.4. Data analysis

The photocatalytic degradation was optimized using response surface methodology (RSM) based on central composite design (CCD). The three factors, solution pH, initial CAF concentration and COD removal, were assessed for two responses, CAF degradation and COD removal. The experimental data were analysed using Design-Expert software version 7.0.0 Stat-Ease (2005).

3. RESULTS AND DISCUSSION

3.1. CAF – TiO_2 dark adsorption and UV photolysis

The probable adsorption of CAF onto the TiO_2 surface was evaluated through dark control tests. A 2 L sample containing 5 mg-CAF/L and 0.5 g-TiO_2 /L, was covered with aluminium foil and kept in the dark for 24 h. The sample pH was maintained at 7.2. Analysis showed that only 9% of the CAF was adsorbed by the catalyst, perhaps because of electrostatic repulsion. This test was conducted to reduce the errors arising from non-photocatalytic adsorption, etc.

UV photolytic experiments were also conducted by irradiating a 2 L sample containing 5 mg-CAF/L for 180 min in the absence of TiO_2. The sample residual CAF concentration was determined after 180 min and CAF removal efficiency was found to be 32%.

3.2. Effect of pH on CAF and COD removal

Figures 2(a) and 2(b) show the effect of pH on CAF photocatalytic degradation. The CAF removal efficiencies obtained at pH 3.0, 5.0, 7.2, and 9.0 were 92.3, 89.1, 86.7, and 60.2%, respectively – that is, CAF photocatalytic degradation was best in acidic solution. This could arise from (i) the surface charge, and/or (ii) the agglomerated photocatalyst sizes.

The isoelectric point (pH_{zc}) is the pH at which a molecule has no net/zero electric charges. The pH_{zc} value of TiO_2 is 6.3. The TiO_2 surface carries a positive charge at low pH, while the charges on CAF and its intermediates are primarily negative and neutral. Thus, at low pH, organic molecule adsorption was facilitated and better photocatalytic degradation was promoted. The photocatalyst also exhibited more photocatalytic activity, due to the greater concentration of hydroxyl radicals. It is noted, too, that TiO_2 particles agglomerate when dispersed in water and that their agglomerated sizes vary from 0.2 to 1.2 μm (Fernandez *et al.* 2014). Particle agglomeration and particle-particle interaction reduce the active sites available for surface holes and electrons, and thus removal efficiency.

3.3. Effect of catalyst dose on CAF and COD removal

Pre-assessment of the optimum photocatalyst dose offers several advantages, including (i) avoiding the use of excess photocatalyst, and (ii) total adsorption of efficient photons. In this study, experiments were conducted with 5 mg-CAF/L initial concentration at pH 7.2, and aliquots were collected every 30 min and analysed for residual CAF concentration. The results are depicted in Figures 2(c) and 2(d).

Increasing the photocatalyst dose from 0.1 to 0.5 g/L raised photocatalytic degradation efficiency from 45.1 to 87.2%. Increasing it further, however, lowered removal efficiency; for example, to 57.8% at 0.9 g/L, because the

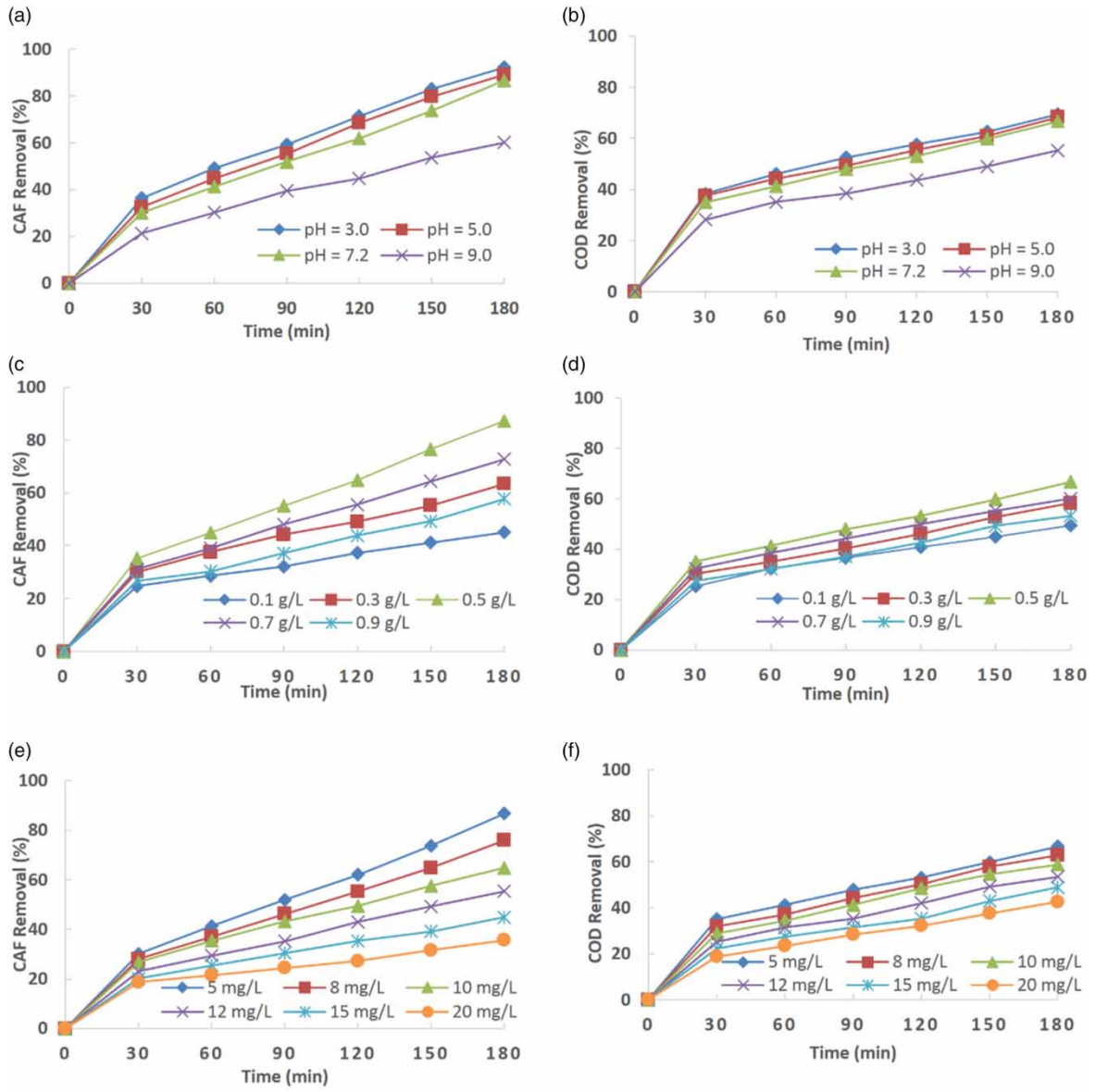

Figure 2 | Effects of feed solution pH, TiO_2 dose, and initial CAF concentration on CAF removal (a), (c) and (e), and COD removal (b), (d) and (f). Standard operating conditions – 5 mg-CAF/L (initial concentration), 0.5 g-TiO_2/L, time 180 min.

excess photocatalyst dose did not facilitate light scattering but reduced light penetration into the reaction mixture (Qourzal *et al.* 2012; Elhalil *et al.* 2018). The optimum catalyst dose of 0.5 g/L was thus chosen for further studies.

3.4. Effect of initial CAF concentration on its removal and kinetics

The effect of initial CAF concentration on its degradation was studied by varying its initial concentration from 5 to 20 mg/L. The experiments were conducted at pH 7.2 with 0.5 g/L catalyst dose (the optimum). The results are shown in Figures 2(e) and 2(f). Hydroxyl radicals are short-lived and exist only for nanoseconds, so that they can only react at or near the location where they are formed. Increasing the CAF concentration increases the probability of collision with the oxidizing species, resulting in an increase in the degradation rate.

The experimental data were fitted to pseudo-first-order kinetics with respect to the CAF concentration – Equations (2) and (3) – as reported by others (Shu *et al.* 2013; Phong & Hur 2015).

$$\frac{d\,[CAF]_t}{dt} = k[CAF]_0 \tag{2}$$

$$ln\frac{[CAF]_0}{[CAF]_t} = -kt \tag{3}$$

where $[CAF]_t$ (mg/L) – the CAF concentration at time t; $[CAF]_0$ (mg/L) – the initial concentration of CAF; t (min) - the reaction time and k (min^{-1}) – the pseudo-first-order rate constant. First-order rate constants were determined by regression analysis and Table 1 shows the constants (k) and R^2 (coefficient of determination) values for different CAF concentrations. The plots for ln $[CAF]_0/[CAF]_t$ and ln $[COD]_0/[COD]_t$ versus t are shown in Figures 3(a) and 3(b). The calculated R^2 values confirmed the pseudo-first-order kinetics removal of CAF. It was also observed that, as the initial concentration increased from 5 to 20 mg/L, the rate constant fell from 0.01 to 0.0021 for CAF degradation and 0.0053 to 0.0028 for COD removal.

Table 1 | Pseudo-first-order kinetic data for CAF degradation and COD removal

	CAF degradation			COD removal	
CAF concentration (mg/L)	K (min^{-1})	R^2	$t_{1/2}$ (min)	K (min^{-1})	R^2
5	0.01	0.9541	69.3	0.0053	0.9367
8	0.0072	0.9757	96.25	0.005	0.9533
10	0.0053	0.9757	130.8	0.0045	0.9563
12	0.0041	0.9756	169	0.0039	0.9526
15	0.0029	0.9473	239	0.0033	0.9488
20	0.0021	0.8957	330	0.0028	0.9515

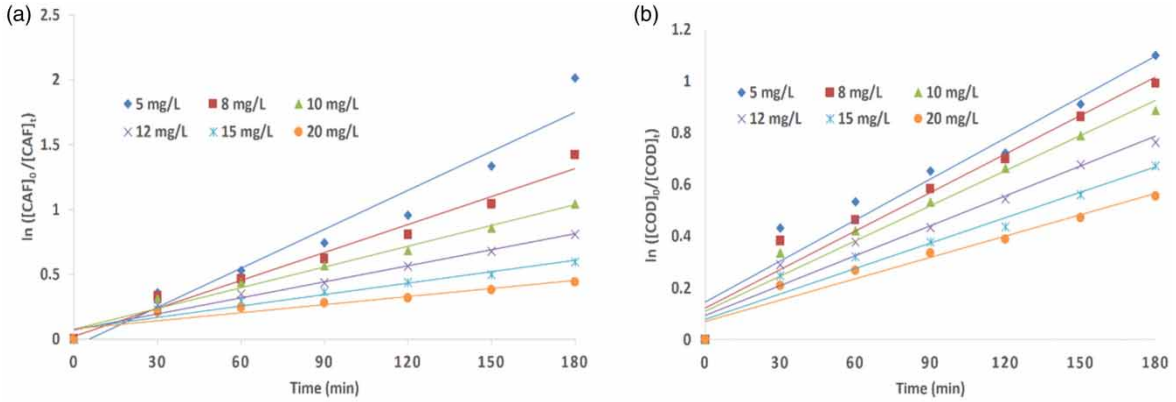

Figure 3 | Pseudo-first-order kinetic plots of (a) ln($[CAF]_0/[CAF]_t$), and (b) ($[COD]_0/[COD]_t$) versus time for CAF.

In pseudo-first-order reactions, the half-life depends on the reaction rate constant and is given by Equation (4).

$$t_{1/2} = \frac{0.693}{k} \tag{4}$$

The k values obtained in this study coincide with the results observed by others (Chuang *et al.* 2011; Luna *et al.* 2018; Mai *et al.* 2018; Sacco *et al.* 2018; Ghosh *et al.* 2019; Muangmora *et al.* 2020). Table 2 shows comparisons of the pseudo-first-order rate constants. The half-life, $t_{1/2}$, determined was 69 min at the optimized concentration of 5 mg-CAF/L. While this coincides with the results obtained by others, Sacco *et al.* (2018) reported $t_{1/2}$ as 92 min and Elhalil *et al.* (2018) reported 87 min.

Table 2 | Literature comparisons for pseudo-first-order rate constants

Citation	Light source	CAF initial concentration (mg/L)	Removal efficiency (%)	K (min^{-1})
Mai *et al.* (2018)	8 W halogen UV lamp	3	100	0.044
Sacco *et al.* (2018)	UV LED 12 W, 365 nm lamp	25	96	0.0075
Muangmora *et al.* (2020)	UV C lamp	5	99	0.0302

3.5. Optimization of operating variables for intensification of CAF degradation and RSM modelling

The interactions between dependent (CAF and COD removal) and independent (initial CAF concentration, catalyst dose and pH) variables were analysed using a quadratic model. For the experimental data, an RSM model with central composite design (CCD) was employed. The experiment parameters and the experimental design are shown in Tables 3 and 4.

The experimental data were thus validated, and the variables' synergistic and antagonistic effects were determined and analysed with the minimum number of experiments. The second-order polynomial equation was

Table 3 | CCD parameters for CAF degradation

Parameter	Symbol	Low (−1)	Center (0)	High (+1)
x_1	CAF concentration (mg/L)	5	12.5	20
x_2	Catalyst dose (g/L)	0.1	0.5	0.9
x_3	pH	3	6	9

Table 4 | Experimental data in CCD for studying CAF photodegradation

Run	Factor 1 A: CAF concentration (mg/L)	Factor 2 B: Catalyst dose (g/L)	Factor 3 C: pH	Response 1 CAF removal (%)	Response 2 COD removal (%)
1	10.00	0.50	7.00	64.8	58.8
2	15.00	0.50	7.00	44.9	43.8
3	5.00	0.30	7.00	63.4	58.2
4	5.00	0.50	3.00	92.3	69.5
5	1.89	0.50	7.00	86.6	66.7
6	12.00	0.50	7.00	55.4	53.3
7	20.00	0.50	7.00	35.6	42.6
8	8.00	0.50	7.00	75.9	62.9
9	5.00	0.50	7.00	87.3	66.7
10	12.50	0.50	9.00	60.2	55.3
11	5.00	0.70	7.00	72.8	60.1
12	5.00	0.10	7.00	45.1	49.4
13	5.00	0.90	7.00	57.8	53.2
14	5.0	0.50	7.00	86.7	66.7
15	12.50	0.50	5.00	89.1	68.3

obtained to describe the correlation between the independent variable and CAF degradation. The ANOVA results for CAF degradation and COD removal are given in Tables 5 and 6.

ANOVA with a high coefficient of determination (R^2) reveals a good agreement between the experimental and predicted values. In this study, ANOVA work yielded R^2 and adjusted R^2 values of 0.9557 and 0.9225, and 0.9369 and 0.8895, respectively, for CAF and COD removal, indicating that the quadratic model is adequate. The degree of freedom (df) indicates the number of estimated parameters used to compute the source's sum of squares. The Model F-value (test for comparing the source's mean square to the residual mean square) of 28.78 for CAF and 19.78 for COD removals obtained in this experiment implies that the model is significant. The 'lack of fit' is the amount by which the model's predictions miss observations. In other words, lack of fit' is the variation of data around the fitted model. It should be insignificant for the model to fit well in the experimental data. The non-significant 'Lack of Fit F-value' of 163.32 and 0.19 obtained for CAF and COD removals indicates that there is a good correlation between process variables and response. The normal plot of residuals and the predicted vs actual response are shown in Figure 4. The residuals fall on a straight line, suggesting that the errors are distributed normally.

Table 5 | ANOVA results for CAF removal efficiency

Source	Sum of Squares	df	Mean Square	F	*p*	
Model	444.85	6	740.98	28.78	<0.0001	Significant
A-CAF concentration	4.43	1	4.43	0.17	0.6892	
B-catalyst dose	121.10	1	121.10	4.70	0.0619	
C-pH	893.22	1	893.22	34.69	0.0004	
AC	589.42	1	589.42	22.89	0.0014	
B^2	1,329.97	1	1,329.97	51.66	<0.0001	
C^2	476.65	1	476.65	18.51	0.0026	
Residual	205.96	8	25.75			
Lack of Fit	205.78	7	29.40	163.32		Not Significant
Pure Error	0.18	1	0.18	0.0602		
Cor Total	4,651.82	14				

Std. Dev.=5.07; Mean=67.86; C.V %=7.48; Adeq Precision=17.08.

Table 6 | ANOVA results for COD removal efficiency

Source	Sum of squares	df	Mean square	F	*p*	
Model	990.88	6	165.15	19.78	0.0002	Significant
A-CAF concentration	0.72	1	0.72	0.086	0.7772	
B-catalyst dose	9.02	1	9.02	1.08	0.3289	
C-pH	208.74	1	208.74	25.00	0.0011	
AC	147.98	1	147.98	17.73	0.0030	
B^2	266.94	1	266.94	31.97	0.0005	
C^2	124.42	1	124.42	14.90	0.0048	
Residual	66.79	8	8.35			
Lack of Fit	66.79	7	9.54	0.19	0.9581	Not Significant
Pure Error	0.000	1	0.000			
Cor Total	1,057.67	14				

Std. Dev.=2.89; Mean=58.37; C.V %=4.95; Adeq Precision=14.445.

The residuals vs predicted, residuals vs run, Box-Cox plot for power transforms, and residuals vs concentration, for both CAF and COD removals, are shown in Figures 5 and 6.

The 3D surface plots are shown in Figure 7. Design-Expert software version 7.0.0 Stat-Ease (2005) with desirability approach was used to predict the maximum CAF and COD removal efficiencies (Stamatis *et al.* 2015). Maximum removal efficiencies were obtained at acidic pH because the surface charge on TiO_2 is then positive. Increasing the TiO_2 dose increased CAF removal efficiency up to 0.5 g-CAF/L, after which it decreased. Light screening and scattering caused the removal efficiency to decrease, while catalyst particle agglomeration also contributed substantially (Antonopoulou *et al.* 2012; Rani & Karthikeyan 2021). Increasing initial CAF concentrations also led to a fall in removal efficiency because the availability of hydroxyl radicals was inadequate.

4. CONCLUSIONS

The photocatalytic degradation of CAF was evaluated in a slurry photocatalytic reactor with intermittent UV irradiation. The highest CAF and COD removals were 86.7 and 66.7% respectively at optimized conditions: CAF=5 mg/L; pH=7.2 and TiO_2=0.5 g/L. CAF and COD removals followed pseudo-first-order kinetics. The experimental data were analysed with RSM modelling, using Design-Expert software. ANOVA yielded R^2=0.9557 and adjusted R^2=0.9225 for CAF removal, and R^2=0.9369 and adjusted R^2=0.8895 for COD removal, confirming good agreement between the experimental and predicted values. The RSM 3D surface plots also

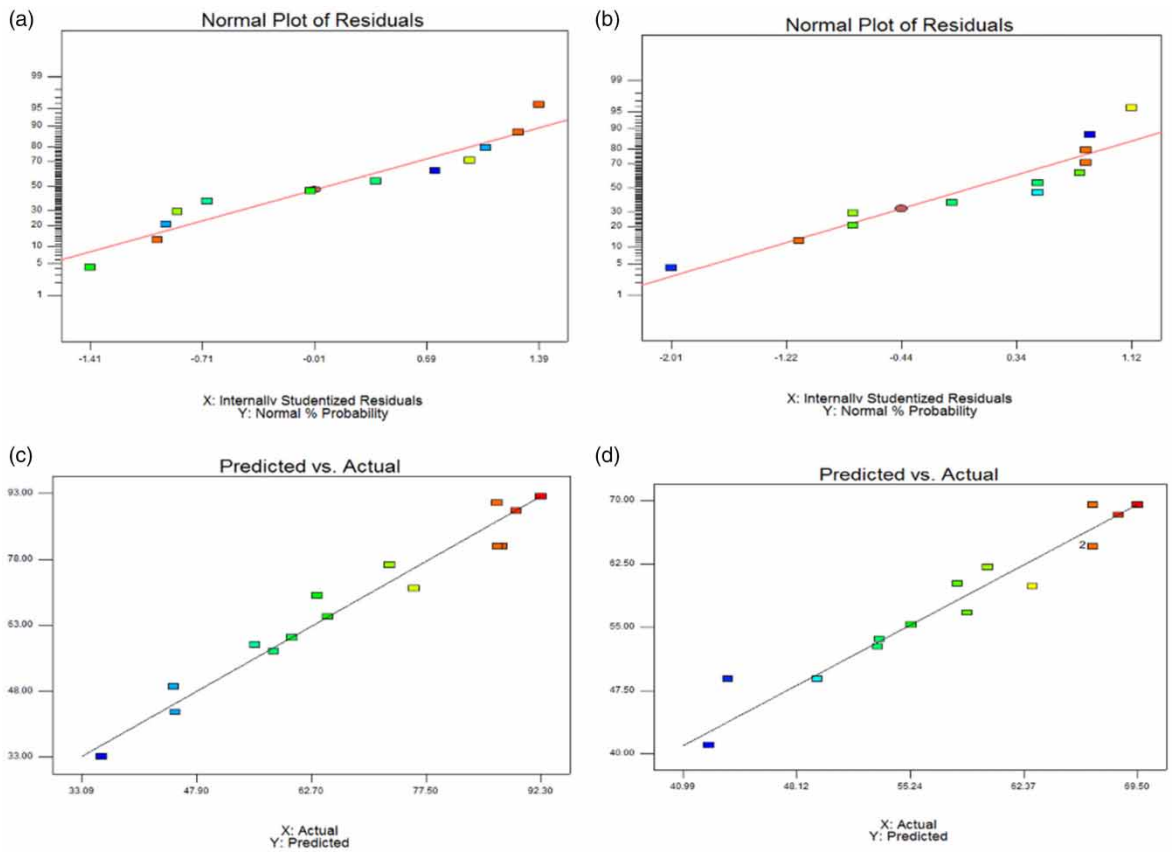

Figure 4 | Normal probability plot of residuals, and predicted vs actual for CAF photocatalytic degradation [(a) & (c)], and COD removal [(b) & (d)].

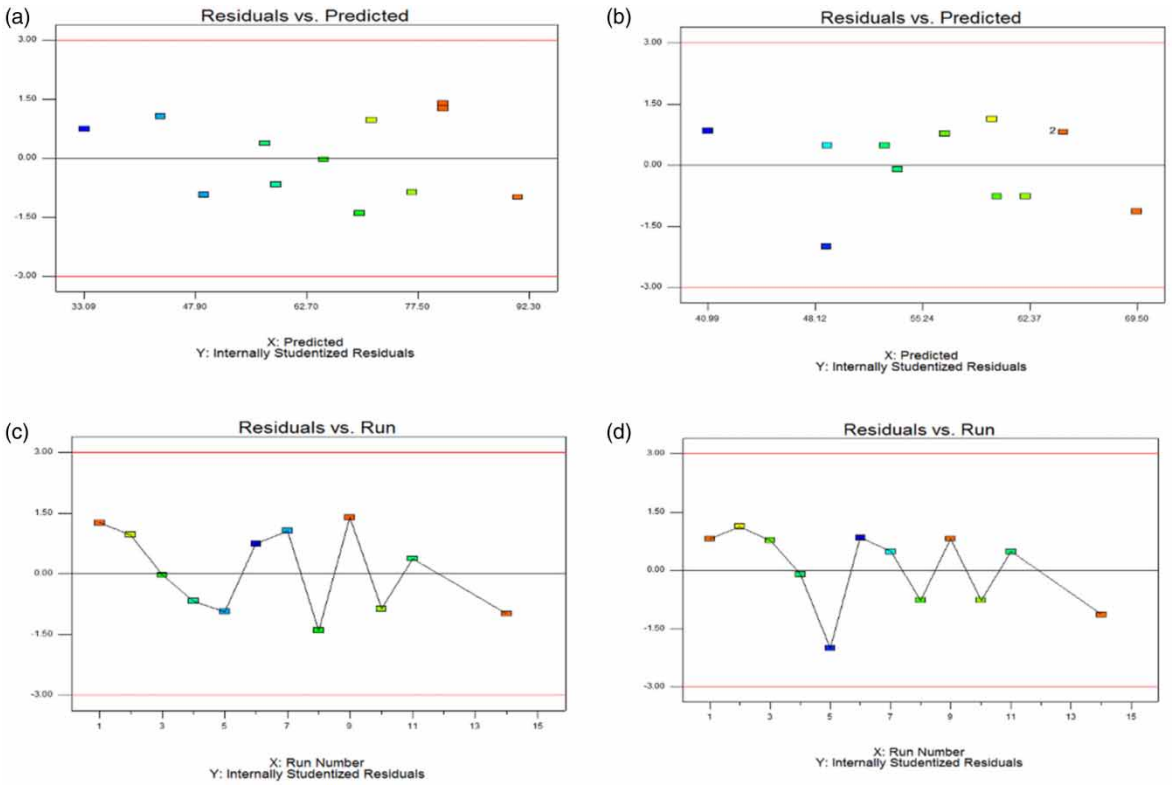

Figure 5 | Residuals vs predicted and residuals vs run photocatalytic values, for CAF degradation [(a) & (c)] and COD removal [(b) & (d)].

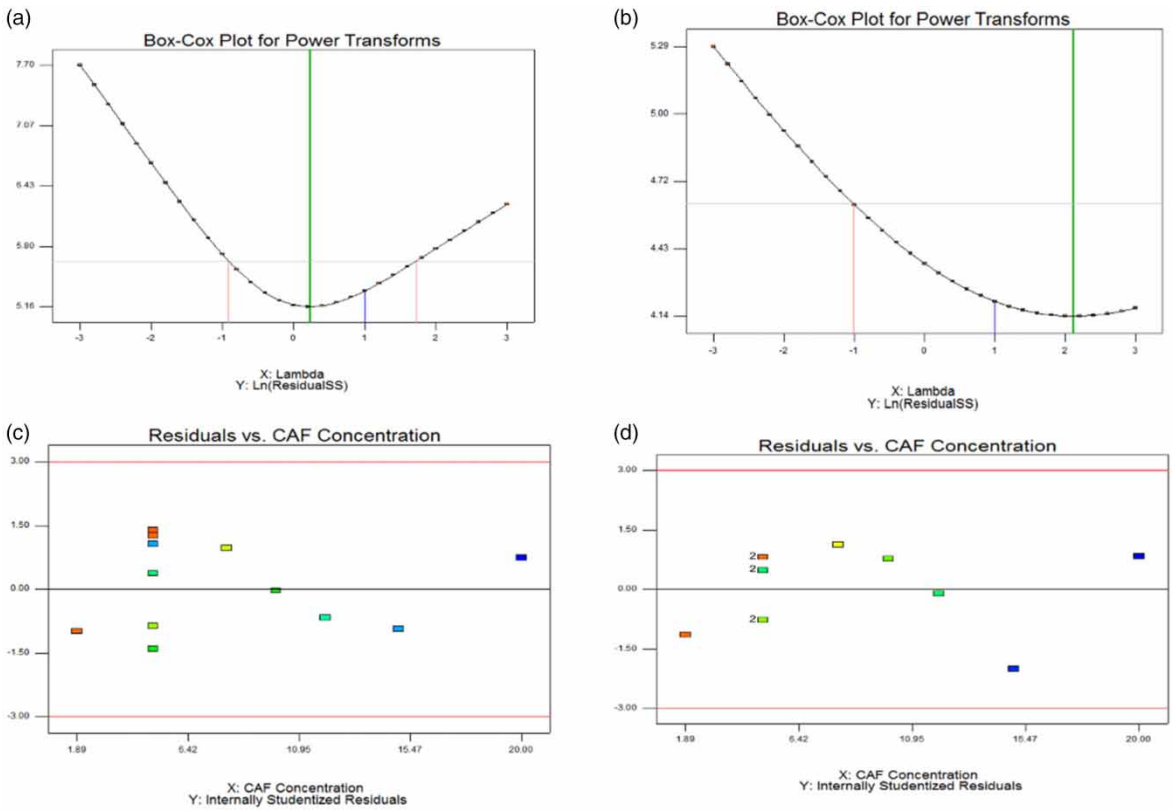

Figure 6 | Box-Cox plot for power transforms and residuals vs CAF concentration, for CAF photocatalytic degradation [(a) & (c)] and COD removal [(b) & (d)].

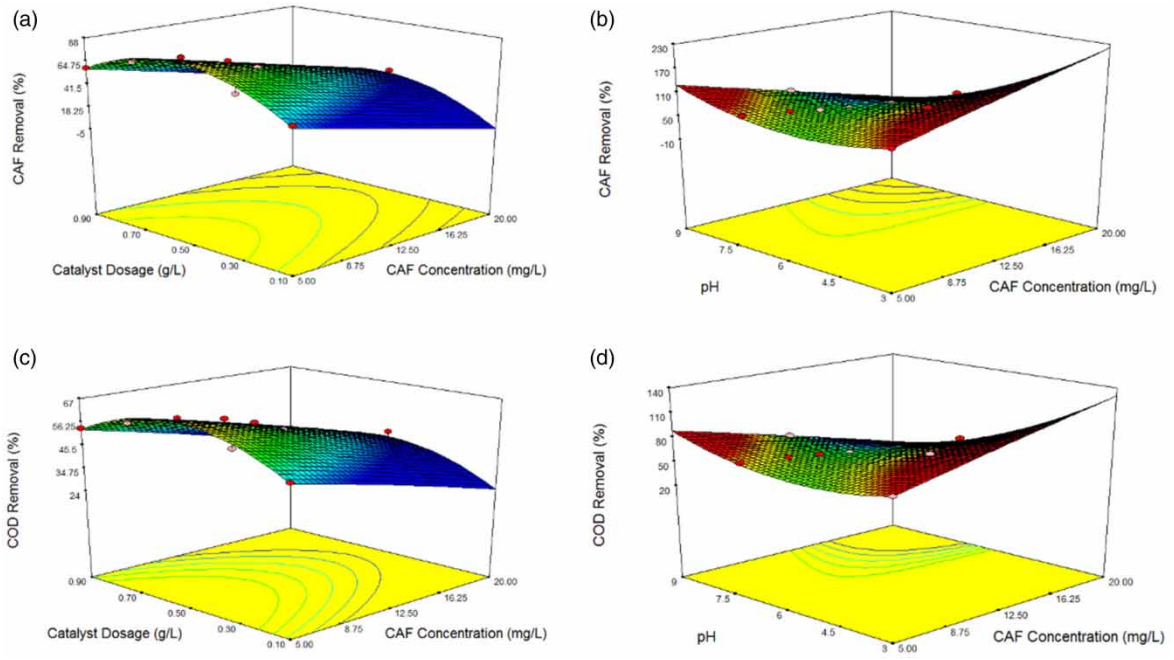

Figure 7 | RSM 3D surface plots for CAF [(a) and (b)] and COD removal [(c) & (d)].

showed that all three operating parameters studied were significant in CAF removal. The study's results also showed that CAF molecules were not degraded completely and COD removal was less than CAF removal.

DATA AVAILABILITY STATEMENT

All relevant data are included in the paper or its Supplementary Information.

REFERENCES

Ahmad, R., Ahmad, Z., Khan, A. U., Mastoi, N. R., Alam, M. & Kim, J. 2016 Photocatalytic systems as an advanced environmental remediation: recent developments, limitations and new avenues for applications. *Journal of Environmental Chemical Engineering* **4**(4), 4143–4164.

Antonopoulou, M., Papadopoulos, V. & Konstantinou, I. 2012 Photocatalytic oxidation of treated municipal wastewaters for the removal of phenolic compounds: optimization and modelling using response surface methodology (RSM) and artificial neural networks (ANNs). *Journal of Chemical Technology and Biotechnology* **87**(10), 1385–1395.

Arfanis, M. K., Adamou, P., Moustakas, N. G., Triantis, T. M., Kontos, A. G. & Falaras, P. 2017 Photocatalytic degradation of salicylic acid and caffeine emerging contaminants using titania nanotubes. *Chemical Engineering Journal* **310**(2), 525–536.

Awfa, D., Ateia, M., Fujii, M., Johnson, M. S. & Yoshimura, C. 2018 Photodegradation of pharmaceuticals and personal care products in water treatment using carbonaceous- TiO_2 composites. A critical review of recent literature. *Water Research* **142**(1), 26–45.

Bahnemann, D. W., Hilgendorff, M. & Memming, R. 1997 Charge carrier dynamics at TiO_2 particles: reactivity of free and trapped holes. *Journal of Physical Chemistry B* **101**(21), 4265–5275.

Barcelo, D. & Petrovic, M. 2008 *Emerging Contaminants From Industrial and Municipal Wastes: Occurrence, Analysis and Effects. The Handbook of Environmental Chemistry*. Springer, Berlin. Heidelberg **5/5S/5S/1**, pp. 1–35.

Bouarioua, A. & Zerdaoui, M. 2017 Photocatalytic activities of TiO_2 layers immobilized on glass substrates by dip-coating technique toward the decolourization of methyl orange as a model organic pollutant. *Journal of Environmental Chemical Engineering* **5**(2), 1565–1574.

Buerge, I. J., Poiger, T., Muller, M. D. & Buser, H. R. 2003 Caffeine an anthropogenic marker for wastewater contamination of surface waters. *Environmental Science and Technology* **37**(4), 691–700.

Chuang, L. C., Luo, C. H., Huang, S. W., Wu, Y. C. & Huang, Y. C. 2011 Photocatalytic degradation mechanism and kinetics of caffeine in aqueous suspension of nano-TiO_2. *Advanced Materials Research* **214**(1), 97–102.

Design Expert, Version 7.0.0 2005 Stat-Ease, Design Expert Inc., Minneapolis. Available from: https://design-expert2.software.informer.com/7.0/.

Diaz-Uribe, C., Vallejo, W. & Romos, W. 2014 Methylene blue photocatalytic mineralization under visible irradiation on TiO_2 thin films doped with chromium. *Applied Surface Science* **319**(1), 121–127.

Edwards, Q. A., Kullikov, S. M. & Garner-O'Neale, L. D. 2015 Caffeine in surface and wastewaters in Barbados, West Indies. *SpringerPlus* **4**(57), 1–12.

Elhalil, A., Elmoubarki, R., Farnane, M., Machrouhi, A., Sadiq, M., Mahjoubi, F., Qourzal, S. & Barka, N. 2018 Photocatalytic degradation of caffeine as a model pharmaceutical pollutant on Mg doped ZnO-Al_2O_3 hetero structure. *Environmental Nanotechnology Monitoring and Management* **10**(1), 63–72.

Fathinia, M. & Khataee, A. 2015 Photocatalytic ozonation of phenazopyridine using TiO_2 nanoparticles coated on ceramic plates: mechanistic studies, degradation intermediates and ecotoxicological assessments. *Applied Catalysis A: General* **491**(1), 136–154.

Fernandez, R. L., McDonald, J. A., Khan, S. J. & Clech, P. L. 2014 Removal of pharmaceuticals and endocrine disrupting chemicals by a submerged membrane photocatalysis reactor (MPR). *Separation Purification and Technology* **127**(1), 131–139.

Fujishima, A., Zhang, X. & Tryk, D. A. 2008 TiO_2 photocatalysis and related surface phenomena. *Surface Science Reports* **63**(12), 515–582.

Gaya, U. I. & Abdullah, A. H. 2008 Heterogeneous photocatalytic degradation of organic contaminants over titanium dioxide: a review of fundamentals, progress and problems. *Journal of Photochemistry and Photobiology C: Photochemistry Reviews* **9**(1), 1–12.

Ghosh, M., Manoli, K., Shen, X., Wang, J. H. & Ray, A. K. 2019 Solar photocatalytic degradation of caffeine with titanium dioxide and zinc oxide nanoparticles. *Journal of Photochemistry and Photobiology A* **377**(1), 1–7.

Gould, J. & Richards, J. 1984 The kinetics and products of the chlorination of caffeine in aqueous solution. *Water Research* **18**(8), 1001–1009.

Indermuhle, C., De Vidales, M., Saez, C., Robles, J., Canizares, P., Garcia-Reyes, J., Molina-Diaz, A., Comninellis, C. & Rodrigo, M. A. 2013 Degradation of caffeine by conductive diamond electrochemical oxidation. *Chemosphere* **93**(9), 1720–1725.

Klamerth, N., Malato, S., Maldonado, M., Aguera, A. & Fernandez-Alba, A. 2010 Application of photo-Fenton as a tertiary treatment of emerging contaminants in municipal wastewater. *Environmental Science and Technology* **44**(5), 1792–1798.

Laohaprapanon, S., Matahum, J., Tayo, L. & You, S.-J. 2015 Photodegradation of reactive black 5 in a ZnO/UV slurry membrane reactor. *Journal of Taiwan Institute of Chemical Engineers* **49**(1), 136–141.

Lovett, R. 2005 Coffee the demon drink? *New Scientist.* **187**, 38–41.

Luna, R., Solis, C., Ortiz, N., Galicia, A., Sandoval, F., Zermeno, B. & Mochezuma, E. 2018 Photocatalytic degradation of caffeine in a solar reactor system. *International Journal of Chemical Reactor Engineering* **16**(10), 1–10.

Mai, L. T., Hoai, L. T. & Tuan, V. A. 2018 Effects of reaction parameters on photodegradation of caffeine over hierarchical flower-like ZnO nanostructure. *Vietnam Journal of Chemistry* **56**(5), 647–653.

Marques, R. R., Sampaio, M. J., Carrapico, P. M., Silva, C. G., Morales-Torres, S., Drazie, G., Faria, J. L. & Silva, A. M. 2013 Photocatalytic degradation of caffeine: developing solutions for emerging pollutants. *Catalysis Today* **209**(1), 10–115.

Miners, J. O. & Birkett, D. J. 1996 The use of caffeine as a metabolic probe for human drug metabolizing enzymes. *General Pharmacology: The Vascular System* **27**(2), 245–249.

Moore, M., Greenway, S., Farris, J. & Guerra, B. 2008 Assessing caffeine as an emerging environmental concern using conventional approaches. *Archives of Environmental Contamination and Toxicology* **54**(1), 31–35.

Mozia, S. 2010 Photocatalytic membrane reactors (PMRs) in water and wastewater treatment. *Separation and Purification Technology* **73**(2), 71–91.

Muangmora, R., Kemacheevakul, P., Punyapalakul, P. & Chuangchote, S. 2020 Enhanced photocatalytic degradation of caffeine using titanium dioxide photocatalyst immobilized on circular glass sheets under ultraviolet C irradiation. *Catalysts* **10**(9), 964.

Pathakoti, K., Manubolu, M. & Hwang, H. M. 2018 Nanotechnology applications for environmental industry. In: *Handbook of Nanomaterials for Industrial Applications*, Vol. 48 (Chaudhery, M. H. ed.). Elsevier, Amsterdam, The Netherlands, pp. 894–907.

Phong, D. D. & Hur, J. 2015 Insight into photocatalytic degradation of dissolved organic matter UVA/TiO_2 systems revealed by fluorescence EEM-PARAFAC. *Water Research* **87**(1), 119–126.

Puga, A. V. 2016 Photocatalytic production of hydrogen from biomass-derived feed stocks. *Coordination Chemistry Reviews* **315**(1), 1–66.

Qourzal, S., Barka, N., Belmouden, M., Abaamrane, A., Alahiane, S., Elouardi, M., Assabbane, A. & Ait-Ichou, Y. 2012 Heterogeneous photocatalytic degradation of 4-nitrophenol on suspended titania surface in a dynamic photo reactor. *Fresenius Environmental Bulletin* **21**(7), 1972–1981.

Rani, C. N. & Karthikeyan, S. 2021 Investigation of naphthalene removal from aqueous solutions in an integrated slurry photocatalytic membrane reactor: effect of operating parameters, identification of intermediates and response surface approach. *Polycyclic Aromatic Compounds* **41**(4), 805–824.

Rimoldi, L., Meroni, D., Falletta, E., Pifferi, V., Falciola, L., Cappelletti, G. & Adizzone, S. 2017 Emerging pollutant mixture mineralization by TiO_2 photocatalysts. The role of the water medium. *Photochemical and Photobiological Sciences* **16**(1), 60–66.

Rosal, R., Rodriguez, A., Perdgon-Melon, J. A., Petre, A., Garia-Calvo, E., Gomez, M. J. A., Aguera, A. & Fernandez-Alba, A. R. 2008 Degradation of caffeine and identification of transformation products generated by ozonation. *Chemosphere* **74**(6), 825–831.

Sacco, O., Vaiano, L., Rizzo, L. & Sannino, D. 2018 Photocatalytic activity of a visible light active structured photocatalyst developed for municipal wastewater treatment. *Journal of Cleaner Production* **175**(1), 38–49.

Shu, Z., Bolton, J. R., Belosevic, M. & El Din, M. G. 2013 Photodegradation of emerging micropollutants using the medium-pressure UV/H_2O_2 advanced oxidation process. *Water Research* **47**(8), 2881–2889.

Souza, F. S. & Feris, L. A. 2015 Degradation of caffeine by advanced oxidative O_3 and O_3/UV. *Ozone: Science and Engineering* **37**(4), 397–384.

Stamatis, N., Antonopoulou, M. & Konstantinou, I. 2015 Photocatalytic degradation kinetics and mechanisms of fungicide tebuconazole in aqueous TiO_2 suspensions. *Catalysis Today* **252**(1), 93–99.

Sudha, D. & Sivakumar, P. 2015 Review on the photocatalytic activity of various composite catalysts. *Chemical Engineering and Processing: Process Intensification* **97**(1), 112–133.

Sujatha, G., Shanthakumar, S. & Chiampo, F. 2020 UV light irradiated photocatalytic degradation of coffee wastewater using TiO_2 as a catalyst. *Environments* **7**(6), 47.

Torres, A. C., Barsan, M. M. & Brett, C. M. A. 2014 Simple electrochemical sensor for caffeine based on carbon and Nafion-modified carbon electrodes. *Food Chemistry* **149**(1), 215–220.

Trovo, A. G., Silva, T. F., Gomes, O., Machado Jr, A. E., Neto, W. B., Muller, P. S. & Daniel Jr, D. 2013 Degradation of caffeine by photo-Fenton process: optimization of treatment conditions using experimental design. *Chemosphere* **90**(2), 170–175.

Vaiano, V., Matarangolo, M. & Sacco, O. 2018 UV-LEDs floating-bed photoreactor for the removal of caffeine and paracetamol using ZnO supported on polystyrene pellets. *Chemical Engineering Journal* **350**(1), 703–713.

Zhang, J., Wang, L. P., Guo, W., Peng, X. D., Li, M. & Yuan, Z. B. 2011 Sensitive differential pulse stripping voltammetry of caffeine in medicines and cola using a sensor based on multi-walled carbon nanotubes and Nafion. *International Journal of Electrochemical Science* **6**(4), 997–1006.

Zhou, P., Xie, Y., Fang, J., Ling, Y., Yu, C., Liu, X., Dai, Y., Qin, Y. & Zhou, D. 2017 Cds quantum dots confined in mesoporous TiO_2 with exceptional photocatalytic performance for degradation of organic pollutants. *Chemosphere* **178**(1), 1–10.

First received 27 October 2021; accepted in revised form 12 December 2021. Available online 24 December 2021